Received: 4 November 2020 | Revised: 30 April 2021 | Accepted: 1 May 2021
DOI: 10.1111/pce.14080

ORIGINAL ARTICLE

Plant, Cell & Environment WILEY

Shifting access to pools of shoot water sustains gas exchange and increases stem hydraulic safety during seasonal atmospheric drought

Callum Bryant[1] | Tomas I. Fuenzalida[1] | Nigel Brothers[1] | Maurizio Mencuccini[2,3] | Lawren Sack[4] | Oliver Binks[1] | Marilyn C. Ball[1]

[1]Plant Science Division, Research School of Biology, Australian National University, Acton, Australia

[2]Catalan Institution for Research and Advanced Studies, Barcelona, Spain

[3]Ecological and Forestry Applications Research Centre, Barcelona, Spain

[4]Department of Ecology and Evolution, University of California Los Angeles, Los Angeles, California

Correspondence
Callum Bryant, Plant Science Division, Research School of Biology, Australian National University, Acton, ACT, 2601, Australia.
Email: callum.bryant@anu.edu.au

Funding information
Australian Research Council Discovery, Grant/Award Numbers: DP170104091, DP180102969

Abstract

Understanding how plants acclimate to drought is crucial for predicting future vulnerability, yet seasonal acclimation of traits that improve drought tolerance in trees remains poorly resolved. We hypothesized that dry season acclimation of leaf and stem traits influencing shoot water storage and hydraulic capacitance would mitigate the drought-associated risks of reduced gas exchange and hydraulic failure in the mangrove *Sonneratia alba*. By late dry season, availability of stored water had shifted within leaves and between leaves and stems. While whole shoot capacitance remained stable, the symplastic fraction of leaf water increased 86%, leaf capacitance increased 104% and stem capacitance declined 80%. Despite declining plant water potentials, leaf and whole plant hydraulic conductance remained unchanged, and midday assimilation rates increased. Further, the available leaf water between the minimum water potential observed and that corresponding to 50% loss of stem conductance increased 111%. Shifting availability of pools of water, within and between organs, maintained leaf water available to buffer periods of increased photosynthesis and losses in stem hydraulic conductivity, mitigating risks of carbon depletion and hydraulic failure during atmospheric drought. Seasonal changes in access to tissue and organ water may have an important role in drought acclimation and avoidance.

KEYWORDS
acclimation, capacitance, drought tolerance, dry season, hydraulic safety margins, leaf, mangrove, pressure-volume curves, shoot, stem

1 | INTRODUCTION

Predicted shifts in rainfall, temperature, and aridity will challenge plant communities across all biomes with atypical drought conditions (Chou et al., 2013; Davy, Esau, Chernokulsky, Outten, & Zilitinkevich, 2017; Ficklin & Novick, 2017; Meehl & Tebaldi, 2004; Trenberth et al., 2014). Drought conditions that exceed species' tolerances reduce plant productivity and increase mortality, with implications for terrestrial water, energy and nutrient fluxes and ecosystem health (Allen & Breshears, 2007; Allen, Breshears, & McDowell, 2015; Yuan et al., 2019). Understanding how plants acclimate to achieve drought tolerance is crucial for predicting future vulnerability (Brodribb, Powers, Cochard, & Choat, 2020).

Droughted plants experience declines in tissue water content (WC) and water potentials (Ψ). While WC and Ψ are positively correlated, their relationship can be non-linear and their effects are distinct (Tyree, Engelbrecht, Vargas, & Kursar, 2003). Declining WC reduces turgor in living cells, inhibits metabolism, and leads to plasmolysis and protoplasm collapse (Hsiao, 1973), whereas declining Ψ increases xylem tension and risk of embolism. For long-lived evergreen plants that cannot avoid periods of environmental drought, strategies for resisting drought diverge along a continuum of desiccation avoidance and tolerance (Kozlowski & Pallardy, 1997; Tyree et al., 2003). Desiccation avoidance traits delay declines in Ψ, whereas desiccation tolerance traits maintain function despite declining Ψ. Further, desiccation tolerant plants may avoid dehydration, that is, by maintaining high WC with declining Ψ, or tolerate dehydration, that is, remain viable despite low WC (Kozlowski & Pallardy, 1997). More frequent stomatal closure to prevent water loss during severe drought reduces gas exchange opportunities, while less frequent stomatal closure increases risks of embolism and loss of stem hydraulic conductance (Adams et al., 2017; Grossiord et al., 2020). Responses to drought determine a species' ability to balance short-term trade-offs (i.e., carbon gain vs. risk of hydraulic damage) with the longer-term competitive trade-offs. The latter may be manifest in differing strategies among neighbouring species sharing a common soil water reservoir, whereby more tolerant species continue to exhaust soil water supplies while neighbouring avoidant species limit water loss (Wolf, Anderegg, & Pacala, 2016). Acclimation to drought within this avoidance-tolerance continuum and its contribution to the mitigation of loss of function remain far from resolved (Brodribb et al., 2020).

Overall, drought resistance is determined by traits coordinated across organs; therefore, identifying changing components contributing to acclimation requires a whole-plant approach (Bartlett, Klein, Jansen, Choat, & Sack, 2016; Blackman et al., 2016; Körner, 2019; Rosas et al., 2019; Sack et al., 2018). Photosynthesis may be prolonged into stressful periods by temporal shifts in stomatal conductance, osmotic adjustment to maintain cell turgor, increased water storage and increased hydraulic capacitance to buffer transpiration demand (Bartlett, Scoffoni, & Sack, 2012; Binks et al., 2016; Nguyen et al., 2017; Sack, Cowan, Jaikumar, & Holbrook, 2003; Scholz, Phillips, Bucci, Meinzer, & Goldstein, 2011). For species that close their stomata to maintain water potentials above dangerous thresholds, the hydraulic safety margin – the margin between minimum water potential (Ψ_{min}) and xylem tensions inducing 50% (P_{50}) or 88% (P_{88}) loss of hydraulic conductance – indexes the relative conservatism of stomatal behaviour with respect to embolism resistance (Meinzer, Johnson, Lachenbruch, McCulloh, & Woodruff, 2009). Across biomes, plants converge on relatively narrow hydraulic safety margins, <1 MPa, and small safety margins increase mortality risk (Anderegg et al., 2016; Choat et al., 2012). Post-stomatal closure, hydraulic safety is also influenced by minimum leaf conductance (g_{min}), whole-plant capacitance, and water storage (Carrasco et al., 2015; Duursma et al., 2019; Gleason, Blackman, Cook, Laws, & Westoby, 2014; Martinez-Vilalta, Anderegg, Sapes, & Sala, 2019).

Water storage (*S*) can be quantified as the absolute WC released over a functional range, that is, the ΔWC between predawn (Ψ_{pd}) and turgor loss (π_{TLP}) or the ΔWC between Ψ_{min} and P_{50}. During persistent drought, Ψ_{pd}, π_{TLP} and Ψ_{min} decline; therefore, *S* may also vary with plant dehydration. Hydraulic capacitance (*C*) for a given organ describes the change in WC or ease of water release for a given change in water potential ($C = \Delta WC/\Delta\Psi$), and is determined using pressure–volume (p–v) curves, that is, plots of water potential (Ψ) against WC. Relationships between WC and Ψ differ among species and among organs (McCulloh, Johnson, Meinzer, & Woodruff, 2014; Scholz et al., 2011). Leaf capacitance (C_{leaf}) may shift with dehydration, and two regions of capacitance can be estimated, a linear region between full turgor and turgor loss and the non-linear region following leaf turgor loss (Bartlett et al., 2012). These two regions of capacitance have distinct roles: (a) when turgor is positive, increased capacitance buffers against changes in Ψ during periods of high transpiration or high vapour pressure difference delaying stomatal closure and loss of leaf hydraulic conductance, and (b) when turgor is lost, increased capacitance may lengthen organ and plant survival by buffering changes in water potential and delaying embolism after stomatal closure (Hao, Sack, Wang, Cao, & Goldstein, 2010; Sack et al., 2003). C_{leaf} is related to other p–v curve parameters, that is, positively to relative water content at turgor loss point ($RWC_{at\ TLP}$), and negatively to the fraction of total extracellular (apoplastic) leaf water (A_f), osmotic potential at full turgor (π_O) and the elastic modulus of the symplast ($\varepsilon_{symplast}$), all of which acclimate to drought (Bartlett et al., 2012, 2014).

Beyond the leaf, the shoot hydraulic capacitance (C_{shoot}), that is, that of leaves and stems combined, determines the water loss required to dehydrate shoots to critical losses of hydraulic conductance (Blackman et al., 2016; Gleason et al., 2014; Martinez-Vilalta et al., 2019). Within shoots, hydraulic segmentation between leaves and stems may also enable hydraulic capacitance to preserve stem hydraulic function at the expense of leaves (Hochberg et al., 2016; Rodriguez-Dominguez, Murphy, Lucani, & Brodribb, 2018). Yet, little is known about the potential for acclimation of *S* and *C* at the scale of the leaf, stem and shoot to both prolong gas exchange and mitigate loss of stem hydraulic function under drought (Körner, 2019; Martinez-Vilalta et al., 2019; McCulloh et al., 2014; Sapes et al., 2019; Scholz et al., 2011).

Here, we explore the role of acclimation of leaf and stem traits in mitigating the twin risks of reduced gas exchange and drought-induced hydraulic failure in the mangrove *Sonneratia alba* Sm. *Sonneratia alba* is a canopy-forming mangrove tree species widespread in the Indo-West Pacific (Duke, Ball, & Ellison, 1998). *S. alba* is an ideal system to study acclimation to atmospheric drought in mangroves as it can be found in locations experiencing strong seasonal atmospheric drought with limited changes in salinity at the roots, a coincidence of its preference for mid-estuarine and low intertidal positions (Duke et al., 1998). We hypothesized that leaf and stem water relations traits would differ between the early and late dry season to (a) maintain levels of photosynthesis, and (b) maintain or increase hydraulic safety margins. Specifically, we hypothesized that drought acclimation of leaf traits such as turgor loss point (π_{TLP}), leaf relative water content at turgor loss point ($RWC_{at\ TLP}$), leaf osmotic potential at full turgor (π_O), elastic modulus (ε), apoplastic fraction (A_f), water storage (*S*) and hydraulic capacitance (*C*) may enhance gas exchange and sustain photosynthesis. In the mitigation of loss of stem hydraulic function, we hypothesized that seasonal acclimation of water storage and hydraulic capacitance of organs of the shoot may increase hydraulic safety margins, with water retention aided by hydraulic segmentation and/or seasonal acclimation of g_{min}.

2 | MATERIALS AND METHODS

2.1 | Study site and sampling design

The study site on the Daintree River, Daintree National Park, Far North Queensland (16°17′24.8″S 145°24′36.8″E), has a tropical monsoonal climate. Long-term monthly rainfall and temperature data were obtained from the Low Isles meteorological station (1968–2017; http://bom.gov.au/climate/data/ accessed March, 2019). Mean annual precipitation for the Daintree region is 2,168 ± 468 mm y^{-1} with ~80% of the rainfall occurring from December through May. Peak mean daily maximum and minimum air temperatures occur in December (32.5 ± 0.9°C) and July (20.5 ± 0.7°C), respectively. Temperature increases and infrequent rainfall over the dry season are associated with progressive increases in daily average vapour pressure deficit (VPD).

Seasonal measurements were conducted early and late in the dry season, 13–25 August and 13–25 November 2018, respectively. Micrometeorological measurements of temperature and relative humidity were recorded at 10 min intervals at the study site during the study period using a portable weather station (Kestrel 3500 Delta T Meter, Neilsen-Kellerman Co., Boothwyn, PA) mounted 3 m above water level at high tide. Shoots with intact healthy, fully expanded foliage, were collected from the same stand of *Sonneratia alba* trees, ~ 6–7 m in height and statistical comparisons were made of mean values. Shoots were sampled at a height ranging from 1.5 to 3 m above high-tide and were transported to the lab in plastic bags with moistened paper towel.

As *S. alba* predominantly grows in loosely consolidated sediments along the estuary margin, the surface water salinities are representative of those experienced by their shallow root systems (Ball & Pidsley, 1995). To assess the estuarine osmotic potentials (Ψ_{est}) experienced by *S. alba*, a handheld refractometer (A.S.T. Co. Ltd., Japan) was used to measure salinity of estuary surface water at high tide. Salinities were averaged from three salinity measurements per day, repeated for each of 5 days during each of the early and late dry season sampling periods. Osmotic potentials of estuarine water were calculated based on the fraction of seawater, where standard seawater has a salinity of 35 ppt and an osmotic potential of −2.4 MPa at 25°C (Harvey, 1966).

2.2 | Leaf and shoot water relations

Leaf water relations were determined from pressure–volume (p–v) curves, that is, plots of leaf water potential versus relative water content (RWC). A p–v curve was constructed for one mature leaf from each of seven trees in the early dry season ($n = 7$) and six trees in the late dry season ($n = 6$) with the bench drying method (Tyree & Hammel, 1972) using a Scholander pressure chamber (1050D, PMS Instrument Albany; Supporting Information). Key leaf traits and water relations parameters were determined, including leaf dry mass per area (LMA), saturated water content (SWC), bulk osmotic potential at turgor loss point (π_{TLP}), relative water content at turgor loss point ($RWC_{at\ TLP}$), osmotic potential at full hydration (π_O), leaf bulk modulus of elasticity (ε), symplastic modulus of elasticity ($\varepsilon_{symplast}$), and fractions of leaf water held in the apoplast (A_f) and symplast (S_f) were calculated from the p–v curves (Bartlett et al., 2012). Capacitance between full turgor and turgor loss (C_{leaf}), for leaves was calculated as:

$$C_{leaf} = \frac{100 - RWC_{TLP}}{0 - \pi_{TLP}} \quad (1)$$

Given that capacitance at leaf water potentials below turgor loss was non-linear, the relationship between RWC and Ψ_{leaf} following turgor loss for p–v curves of each season was estimated from using the linear relationships between RWC and $1/\Psi_{leaf}$ following turgor loss (Figure S1). Capacitance at a given water potential following turgor loss was estimated by the deriving the tangent line of the changing relationship between RWC and Ψ_{leaf} (i.e., $\Delta RWC/\Delta\Psi_{leaf}$; Bartlett, Detto, & Pacala, 2019).

To assess the relative capacitance (*C*) of shoots, stems and leaves, shoot pressure-volume curves were constructed in the early and late dry season using a modified bench drying method (Gleason et al., 2014). One shoot, >60 cm in length, was cut from each of four trees in the early dry season and five trees in the late dry season in the late afternoon, each with several dozen leaves. Upon return to the lab, these shoots were recut under perfusion solution of 1% seawater (~0.02 MPa) and rehydrated overnight. Upon rehydration to > −0.5 MPa, terminal shoots were re-cut, weighed, and shoot water potential (Ψ_{shoot}) was determined as the average Ψ_{leaf} of two leaves, measured using a pressure chamber. Shoots were then allowed to bench dry, permitting sufficient time for Ψ_{shoot} to decline ~0.5 MPa, after which the shoots were incubated in black plastic bags for 40–90 min, to allow equilibration. Shoots were then re-weighed before and after measurement of Ψ_{shoot} as above. This sequence was repeated and records were kept to account for the decline in fresh mass due to repeated removal of leaves for determination of Ψ_{shoot} after each drying interval, and determining the dry mass of removed leaves, and of the remaining stems and leaves and stems after oven drying for >72 h at 70°C. From these data, the shoot water content (WC; $g_{water}\ g^{-1}{}_{dry\ mass}$) and RWC was determined throughout the dehydration, yielding a shoot p–v curve. The leaf water fraction of shoot water was determined from leaf capacitance ($g_{water\ released}\ g^{-1}{}_{dry\ mass}\ MPa^{-1}$) derived from the leaf p–v curves based on the $\Delta\Psi$ for each dehydration interval. Leaf water content was then subtracted from total shoot water content to determine the stem water content during shoot dehydration, yielding a stem p–v curve. For shoots and stems, *C* was then calculated from the linear slope describing the decline in water content with the decrease in shoot water potential during the initial linear part of the slope.

2.3 | Diurnal hydraulic function and gas exchange characteristics

Diurnal changes in stem and leaf water status, gas exchange and leaf hydraulic conductance were monitored in five co-occurring trees in both the early and late dry season. Diurnal measurements of Ψ_{leaf} and stem water potential (Ψ_{stem}) were measured over three clear sunny days (with no leaf wetting on the preceding evening) in the early dry season (August 19–21) at 6:00 (predawn; Ψ_{pd}), 9:00 (morning), 12:00 (midday), and 15:00 h (afternoon), and on one clear sunny day in the late dry season (November 22) at 5:00 (predawn; Ψ_{pd}), 8:00 (morning), 11:00 (midday), 14:00 (afternoon) and 17:00 h. Sampling times were shifted forward 1 h between seasons to standardize comparisons of morning, midday and afternoon measurements based on hours from sunrise, which differed between seasons. Sunrise occurred at 6:35 a.m. and 5:38 a.m. for early and late dry season respectively. Ψ_{stem} was determined in leaves wrapped in plastic film and aluminium foil and allowed to equilibrate with the stem (Melcher, Meinzer, Yount, Goldstein, & Zimmermann, 1998; Supporting Information). Gas exchange measurements were made using a portable photosynthesis system (LI-COR 6400XT, LI-COR Biosciences, Nebraska). Photosynthetically active radiation was standardized at 1000 μmol photons m^{-2} s^{-1} and the flow rate was set to 500 μmol s^{-1}, and all other parameters (CO_2, temperature, humidity) were left at ambient levels. After attaching the gas analyser head, measurements were logged after photosynthetic rate and stomatal conductance stabilized (usually 2–3 min). The time elapsed between the first tree and last tree during a measurement cycle was <45 min. After gas exchange measurements, the exposed and the wrapped leaves were harvested, placed into zip-lock bags and their water potentials measured in the lab within 90 min. Leaf hydraulic conductance (K_{leaf}) was calculated from diurnal gas exchange and water potential measurements on an area basis as:

$$K_{leaf} = \frac{E}{(\Psi_{stem} - \Psi_{leaf})} \quad (2)$$

where E is the transpiration rate and Ψ_{stem} - Ψ_{leaf} represents the water potential gradient between the transpiring leaf and stem. Similarly, whole-plant conductance (K_{plant}) was calculated on a leaf area basis as:

$$K_{plant} = \frac{E}{(\Psi_{est} - \Psi_{leaf})} \quad (3)$$

where Ψ_{est} is the estuarine water potential. To assess seasonal changes in the hydraulic resistance in the roots and stem due to drought, the sum of stem and root resistance was obtained by subtracting leaf from whole plant resistance (Tsuda & Tyree, 1997; Supporting Information).

Minimum leaf conductance (g_{min}), was determined for leaves from each of nine trees in the early dry season and five in the late dry season. Minimal leaf conductance, g_{min}, was determined by methods previously described (Kerstiens, 1996; Sack et al., 2003) as the cuticular transpiration, per two sided area, per mole fraction difference in water vapour between leaf and air, where air inside the leaf was assumed saturated with water vapour (Pearcy et al., 2000; Supporting Information).

2.4 | Hydraulic vulnerability

The relationship between K_{leaf} (leaf hydraulic conductance via the petiole) and declining leaf water status (Ψ_{leaf}) was determined using the rehydration kinetics method (Brodribb & Holbrook, 2003). The relationship of stomatal conductance to Ψ_{leaf} was plotted using paired measurements of gas exchange and Ψ_{leaf} made in the late dry season. Early dry season measurements were not included in g_s response curves as seasonal differences in modes of diurnal gas exchange were observed between early and late dry season. In the early dry season, stomatal conductance was moderate throughout the day, whereas in the late dry season, stomatal conductance was characterized by high values in the morning followed by rapid decline with declining water status in the afternoon.

Loss of stem hydraulic conductivity with declining water potential (Ψ_{stem}) was estimated in the early dry season using the pneumatic method (Pereira et al., 2016; Zhang et al., 2018). Maximum vessel length was determined for shoots from five trees by supplying the basal end of a cut branch with air under low positive pressure, and making progressive cuts at the distal, submerged end of the branch until air was discharged from the distal end, indicating the longest vessel had been cut. The length of the remaining branch was determined with a measuring tape (Ewers & Fisher, 1989). Maximum vessel length was 47 ± 1 cm; subsequently, pneumatic curves were constructed for shoots >60 cm in length, from each of six trees (Supporting Information).

K_{stem}, K_{leaf} and g_s values, were plotted against Ψ values for measurements and fitted with a re-parameterized Weibull model (Ogle, Barber, Willson, & Thompson, 2009; Supporting Information). Leaf or stem water potentials corresponding to 12% (P_{12}), 50% (P_{50}) and 88% (P_{88}) loss of conductance were estimated and, where sample size permitted, 95% bootstrap confidence intervals were generated with 1,000 resamples using the *fitplc* package in R (cran.r-project.org/package=fitplc). Measurements from all shoots were pooled and random effects associated with individual shoots factored into estimates and confidence intervals using the *random effects* argument of the *fitplc* package. Strength of modelled fits were assessed by plotting curve predictions of conductance against observed conductance, and significance of correlations were assessed with linear models.

Hydraulic vulnerability segmentation was assessed using hydraulic safety margins HSM calculated for leaves and stems (Choat et al., 2012; Supporting Information). The minimum leaf and stem water potential were determined as the lowest diurnal measurements for each sampling period. While hydraulic safety margins are conventionally assessed in terms of Ψ, by combining data from leaf pressure-volume curves and hydraulic safety margins, we also assessed this hydraulic safety margins in terms of absolute leaf water available to buffer exposure to stem P_{50} as:

$$HSM_{50\,stem} = SWC\,(RWC_{leaf\ at\ \Psi min} - RWC_{leaf\ at\ stem\ P50}) \quad (4)$$

2.5 | Analyses

Statistical analyses were performed using R (Version 3.6.1, R Core Team, 2019). Early and late dry season differences in site conditions, leaf traits and hydraulic safety margins were assessed with two-tailed *t*-tests, after an *F*-test was conducted to test for equal variance. Seasonal contributions of leaves and stem water to shoot capacitance were analysed using two-way repeated measures ANOVAs in R with the NLME package, with organ and season given as predictor variables. Similarly, diurnal hydraulics and gas exchange measurements were analysed using two-way repeated measures with time of day (standardized between seasons as morning, midday and afternoon) and season as predictor variables. Where applicable, post hoc pairwise comparisons were performed using Tukey's HSD with the EMMEANS package for R. All results given in the text are mean values ± SE, or, mean values and upper and lower confidence limits at 95%. In calculations involving the integration of two methods, that is, partitioning of shoot capacitance and expressing hydraulic safety margins in terms of leaf water content, error associated with the mean value of a given parameter was propagated through calculations by adding error in quadrature. Regression lines required to derive parameters or assess correlations were evaluated with standard major axis regression using the SMATR package for R.

3 | RESULTS

3.1 | Drought responses and shifts in water relations parameters

Between early and late dry season, predawn leaf water potentials declined by 1.08 ± 0.09 MPa (Table 1, $p < .001$). In the early dry season leaf and stem water potentials were equilibrated with estuarine water potential before dawn, but in the late dry season, we observed a 0.93 ± 0.08 MPa predawn disequilibrium between leaf and estuarine water potentials (Table 1, $p < .001$). Estuarine salinity increased from 66.9 ± 0.8% to 72.6 ± 0.5% seawater from the early to the late dry season ($p < .01$, Table 1), corresponding to osmotic potentials of −1.61 ± 0.02 and − 1.74 ± 0.01 MPa, respectively. Daily average VPD increased from 0.64 ± 0.04 to 1.14 ± 0.07 kPa from the early to late dry season ($p < .001$, Table 1).

We observed declines in leaf osmotic potentials at full turgor (π_O) and zero turgor (π_{TLP}) and in bulk relative water content at turgor loss point ($RWC_{at\ TLP}$; all $p < .01$, Table 1). The magnitude of the osmotic adjustment at full turgor (−0.66 ± 0.15 MPa) did not correspond to the decrease in estuarine osmotic potential which was relatively small (−0.13 ± 0.04 MPa). Between early and late dry season leaf capacitance above turgor loss point increased by 104 ± 17% ($g_{water}\ g^{-1}{}_{dry\ mass}$ MPa $^{-1}$, $p < .001$, Table 1). Leaf dry mass per unit area declined by 15 ± 5% between early and late dry season ($p < .001$), together with a 15 ± 3% increase in saturated leaf water content per dry mass ($p < .01$). The fraction of water stored in the apoplast declined 38 ± 7%, corresponding to an 87 ± 16% increase in the symplastic water content between early and late dry seasons ($p < .001$, Table 1). While a significant decline in bulk elastic modulus was observed, no difference was found when this variable was calculated using only the decline in symplastic water (Table 1, Bartlett et al., 2012). The relative symplastic water content at leaf turgor loss point did not differ between seasons (∼76 ± 3% RWC). Shoot water content at full hydration was statistically similar between early and late dry season, as was shoot capacitance (∼5.0 ± 0.7% RWC_{shoot} MPa^{-1}, Table 2). The leaf contribution to shoot capacitance increased from 3.2 ± 0.3% to 4.0 ± 0.3% RWC_{shoot} MPa^{-1} between early and late dry season ($p < .001$, Table 2). Stem contribution to shoot capacitance declined from 2.2 ± 0.3% to 0.07 ± 0.3% RWC_{shoot} MPa^{-1} ($p < .001$, Figure 1, Table 2).

3.2 | Diurnal hydraulic function and shifts in gas exchange characteristics

In both the early and late dry season, Ψ_{leaf} declined progressively throughout the day, by late dry season $\Psi_{min\ leaf}$ reached π_{TLP} (Figure 2a, Tables 1 and 4). Between early and late dry season, minimum water potentials decreased in leaves and stems by 0.96 ± 0.06 MPa and 0.62 ± 0.08, respectively (Figure 2a,b, Table 4). The average water potential difference between Ψ_{leaf} and Ψ_{stem} during the day increased by 0.17 ± 0.09 MPa ($p < .001$) between early dry season (0.24 ± 0.04 MPa) and late dry season (0.41 ± 0.09 MPa). Despite declining plant water potentials and increased hydraulic tension, no significant declines in K_{leaf} and K_{plant} were observed between early and late dry season in morning, midday, and afternoon measurements (Figure 2c,d) and the hydraulic resistance of the roots and stems were statistically similar (Figure S2a,b). An additional time point, 17:00, was measured in the late dry season only, demonstrating declines in g_s, K_{leaf} and K_{plant} throughout the day in the late dry season.

We observed strong shifts between early and late dry season in CO_2 assimilation rates (*A*) and stomatal conductance (g_s; Figure 2e,f). Midday *A* increased in the late dry season ($p < 0.05$). Morning and midday g_s were greater in late dry season ($p < .05$ and $p < .01$ respectively, Figure 4b), however, net daily assimilation may have been offset by the trend towards declining *A* in late afternoon. Increases in g_s and *A* occurred despite higher day and night-time vapour pressure deficit in the late dry season averaged over 12 days of micrometeorological data, and specifically during gas exchange measurements (Figures S2c, d). Minimum leaf conductance was statistically similar between the seasons (Table 1).

3.3 | Mitigation of hydraulic failure

Late dry season stem hydraulic function was conserved by early stomatal closure, hydraulic segmentation between leaves and stems and large hydraulic safety margins. Stomatal closure was only observed in the late afternoon in the late dry season, co-occurring with declines in whole plant conductance. The onset of stomatal closure, that is, g_{s12} and g_{s50}, occurred at lower Ψ_{leaf} than P_{12} and P_{50} for K_{leaf} (Table 3). However, the slope (S_x) of decline in stomatal conductance at P_{50} (S_x) with declining water status was greater than that of K_{leaf}

TABLE 1 Dry season changes in site conditions, physical leaf traits, water relations and minimal leaf conductance

Parameter	Symbol	Early dry season $n = 7$	Late dry season $n = 6$
Site conditions			
Estuarine salinity (% seawater)	-	66.9 ± 0.8	72.6 ± 0.5 *
Estuarine osmotic potential (MPa)	Ψ_{est}	−1.61 ± 0.02	−1.74 ± 0.02 *
Vapour pressure deficit (mean kPa)	VPD	0.64 ± 0.04	1.14 ± 0.07 ***
Leaf predawn water potential (MPa)	$\Psi_{pd\ leaf}$	−1.59 ± 0.04	−2.67 ± 0.08 ***
Stem predawn water potential (MPa)	$\Psi_{pd\ stem}$	−1.56 ± 0.02	−2.57 ± 0.04 ***
Physical traits			
Leaf area (cm^{-2})	-	29.8 ± 0.1	22.2 ± 0.1*
Leaf dry mass per area ($g\ m^{-2}$)	LMA	209.9 ± 8.7	178.2 ± 5.3 **
Leaf saturated fresh mass ($g\ m^{-2}$)	Fm	671 ± 28	660 ± 6 ns
Saturated leaf water content per unit area ($g_{water}\ m^{-2}$)	SWC_{area}	473 ± 5	465 ± 20 ns
Saturated leaf water content per gram ($g_{water}\ g_{dry\ mass}^{-1}$)	SWC_{dm}	2.30 ± 0.06	2.64 ± 0.05 **
Leaf water relations			
Bulk turgor loss point (MPa)	π_{TLP}	−2.87 ± 0.05	−3.42 ± 0.07 ***
Relative water content at turgor loss point (%)	$RWC_{at\ TLP}$	88.6 ± 0.3	78.8 ± 0.7 ***
Symplastic relative water content at turgor loss point (%)	$RWC_{symplast\ at\ TLP}$	75.8 ± 1.9	76.0 ± 2.8 ns
Solute potential at full hydration (MPa)	π_O	−1.95 ± 0.07	−2.38 ± 0.12 *
Bulk leaf capacitance Relative capacitance (Δ *RWC* MPa^{-1})	C_{leaf}	3.63 ± 0.18	5.85 ± 0.27 ***
Mass specific capacitance ($g_{water}\ g^{-1}_{dry\ mass}\ MPa^{-1}$)	C_{leaf}	0.083 ± 0.005	0.170 ± 0.010 ***
Leaf water storage capacity from saturation to π_{TLP} ($g_{water}\ m^{-2}$)	S	49.3 ± 2.6	93.0 ± 6.2 ***
Leaf water storage available predawn to π_{TLP} ($g_{water}\ m^{-2}$)	S	21.7 ± 1.7	21.0 ± 2.5 ns
Modulus of elasticity (MPa)	ε	21.5 ± 1.0	13.1 ± 0.7 ***
	$\varepsilon_{symplast}$	11.9 ± 1.3	9.7 ± 1.0 ns
Apoplastic fraction (% bulk leaf RWC)	A_f	56.0 ± 3.3	17.7 ± 6.0 ***
Symplastic fraction (% bulk leaf RWC)	S_f	44.0 ± 3.3	82.3 ± 6.0 ***
Minimum leaf conductance ($mmol\ m^{-2}\ s^{-1}$)	g_{min}	2.95 ± 0.14	3.12 ± 0.38 ns

Note: Values are means ± SE, see top row for respective *n*. Significance codes: * ($p < .05$), ** ($p < .01$), *** ($p < .001$) between early and late dry season.
Abbreviations: LMA, leaf dry mass per area; RWC, relative water content; VPD, vapour pressure deficit.

TABLE 2 Parameters derived from terminal shoot water-release curves

Parameter	Season	Shoot	Leaves	Stem
RWC at full hydration (% RWC_{shoot})	Early	100	64.2 ± 2.8	34.5 ± 2.8
	Late	100	59.2 ± 3.6	39.3 ± 3.8
WC at full hydration ($g\ g^{-1}$ dry mass)	Early	2.32 ± 0.15	2.29 ± 0.04	2.44 ± 0.43
	Late	2.22 ± 0.09	2.68 ± 0.02	1.77 ± 0.14
C (Δ RWC_{shoot} MPa^{-1})	Early	5.4 ± 0.6	3.2 ± 0.3	2.2 ± 0.3
	Late	4.6 ± 0.3	4.0 ± 0.3	0.7 ± 0.3
C ($g_{water}\ g^{-1}_{dry\ mass}\ MPa^{-1}$)	Early	0.12 ± 0.01	0.08 ± 0.01	0.20 ± 0.05
	Late	0.10 ± 0.01	0.17 ± 0.01	0.04 ± 0.01
RWC at leaf π_{TLP} (% RWC_{shoot})	Early	83.4 ± 1.6	55.4 ± 2.2	28.3 ± 3.3
	Late	84.1 ± 1.8	46.4 ± 2.5	37.6 ± 3.5

Abbreviation: RWC, relative water content.

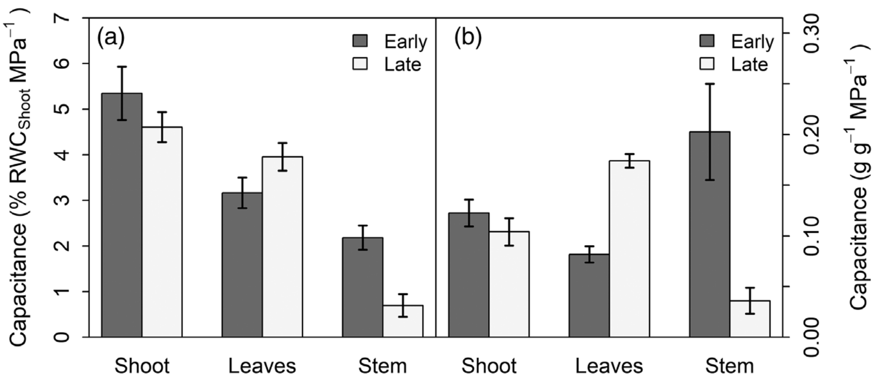

FIGURE 1 (a) Dry season acclimation of contribution of organs (leaves and stems) to shoot capacitance (two-way repeated measures ANOVA: significant effects for organ ($F_9 = 84.55$, $p < .001$); no significant effect for season ($F_9 = 1.96$, $p = .19$); significant organ × season interaction ($F_9 = 21.43$, $p < .001$). (b) Dry season acclimation of shoot, leaf, and stem capacitance and per gram organ dry mass (two-way repeated measures ANOVA: no effect for organ or season, but significant organ × season interaction [$F_9 = 33.35$, $p < .001$]).
Note: Leaf capacitance depicted in (b) is derived from leaf PV curves, Table 1. Data are presented as means ± SE

($p < .05$, Table 3, Figure 3), suggesting declines in K_{leaf} were outpaced by stomatal closure. The water potential associated with 50% loss of stomatal conductance, −3.10 MPa (−3.25, −2.93; 95% CL), preceded late dry season leaf turgor loss point (−3.42 ± 0.07 MPa). Estimates of P_{12}, P_{50} and P_{88} were higher in leaves than in stems ($p < .001$, Table 3). The water potential associated with 95% loss of $K_{leaf,}$ −6.00 MPa (−4.86, 95% CL), did not differ significantly from P_{50} in stems, −5.92 MPa (−5.41, −6.49; 95% CL).

Due to declining minimum water potentials, the hydraulic safety margins to loss of 50% conductance were lower for the late than early dry season in leaves and stems (estimates summarized in Table 4). Hydraulic safety margins were larger in stems than in leaves. Leaves had negative mean HSM_{50} in the late dry season of −1.26 MPa, yet maintained a positive mean HSM_{88} of 1.21 MPa. Stems had consistently positive HSM_{50} and HSM_{88} and larger relative to leaves, with mean values of 2.87 and 4.19 MPa, respectively ($p < .001$ for both HSM_{50} and HSM_{88}).

Finally, we assessed seasonal differences in the capacity of leaf water available to buffer exposure to water potentials associated with stem P_{50}. $HSM_{50,}$ when expressed in terms of leaf water released between Ψ_{min} and stem $P_{50,}$ increased from 13.8 ± 3.2% RWC to 27.8 ± 4.3% RWC in the late dry season ($p < .05$, Table 4). This is equivalent to a doubling of absolute leaf water available between Ψ_{min} and stem P_{50}, from 0.063 ± 0.0137 kg m^{-2} to 0.133 ± 0.015 kg m^{-2} ($p < .05$, Table 4). Counterintuitively, this increase in available leaf water occurred despite increasingly negative daily plant water potentials as the dry season progressed (Figure 4). Increased C_{leaf} resulted in significantly lower leaf bulk RWC at Ψ_{min} in the late dry season (76.0 ± 2.6%) compared to the early dry season (90.0 ± 1.6%). Similarly, increase in C_{leaf} after turgor loss also resulted in significantly lower leaf bulk RWC at water potentials associated with stem P_{50} in late dry season (48.1 ± 3.4%) relative to early dry season (76.2 ± 2.8%). However, despite increased release of bulk leaf water, $RWC_{symplast\ at\ TLP}$ and $RWC_{symplast\ at\ stem\ P50}$ were not significantly different between early and late dry season (Tables 1 and 4).

4 | DISCUSSION

We found strong coordinated dry season acclimation in many water relations traits to the predominately atmospheric drought experienced in the field by the mangrove *Sonneratia alba*. Changes in the location and ease of release of pools of water within the plant sustained gas exchange in the late dry season, while also mitigating risk of stem hydraulic failure. Within leaves, increases in the symplastic fraction of water combined with decreases in solute potential prolonged turgor, increased C_{leaf}, buffered changes in leaf $RWC_{symplast}$, and maintained the absolute shoot water available to buffer transpiration demand between Ψ_{pd} and π_{TLP}. Further, despite declining tissue water potentials, increased C_{leaf} offset seasonal declines in stem capacitance conserving overall shoot capacitance as well as doubling the potential leaf water available to buffer changes in Ψ_{stem} between Ψ_{min} and $P_{50\ stem}$.

4.1 | Shifting access to pools of water within leaves driven by changes in A_f and π_O

Increases in leaf capacitance are causally driven by lower $\varepsilon_{symplast}$ and A_f, more negative π_O, and increases in SWC_{area} (Bartlett et al., 2012). In *S. alba*, $\varepsilon_{symplast}$ and SWC_{area} did not change between seasons, therefore increases in C_{leaf} appear predominately associated with declining π_O in conjunction with a 38 ± 7% reduction in the A_f (Table 1). While declining π_O under drought conditions has been widely documented (Bartlett et al., 2012; Sanders & Arndt, 2012), the direction of A_f acclimation among species under drought conditions appears mixed, with large reversible increases observed in *Psuedotsuga menzieii* (Joly & Zaerr, 1987), and both increases and decreases observed among sunflower genotypes (Chimenti & Hall, 1994; Maury, Berger, Mojayad, & Planchon, 2000). In *S. alba*, declines in $A_{f,}$ despite a seasonally conserved $SWC_{area,}$ suggest increased C_{leaf} involved expansion of absolute symplastic water content. In the late dry season, *S. alba* leaves also had lower leaf dry mass

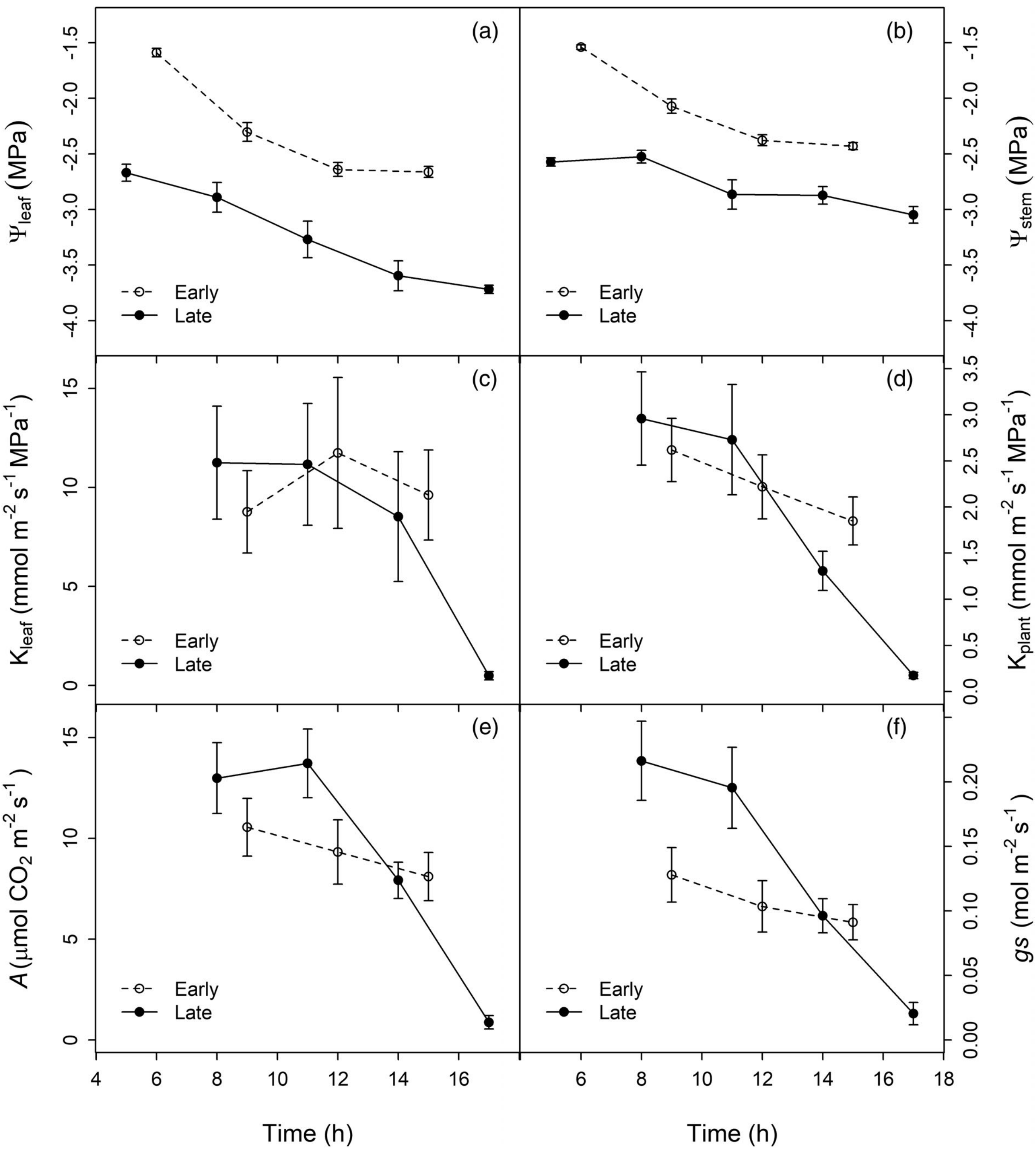

FIGURE 2 Late dry season maintenance of hydraulic conductance and gas exchange despite declining water potentials. (a) Dry season declines in diurnal leaf (Ψ_{leaf}) and (b) stem (Ψ_{stem}) water potential. (c) Maintenance of diurnal leaf (K_{leaf}) and (d) whole plant (K_{plant}) hydraulic conductance (e) Dry season shift in diurnal photosynthetic assimilation rates (*A*; two-way repeated measures ANOVA: significant effects for time of day ($F_{18} = 5.06$, $p = .02$) and season ($F_{18} = 5.30$, $p = .03$); but no season × time interaction ($F_{18} = 1.43$, $p = .26$)). (f) Dry season shift in diurnal stomatal conductance (g_s; two-way repeated measures ANOVA: significant effects for time of day ($F_{18} = 6.52$, $p = .01$) and season ($F_{18} = 15.38$, $p = .001$); but no season × time interaction ($F_{18} = 3.07$, $p = .07$).
Note: late dry season declines of K_{leaf} and K_{plant} cannot be distinguished from declines in g_s due to their measurement with the trans-flux method (Melcher et al., 1998). Data are presented as means ± SE, $n = 5$

per unit area, lower ε and higher SWC_{dm} (Table 1), all of which suggest increased leaf succulence (Bartlett et al., 2012; Ogburn & Edwards, 2010; Vendramini et al., 2002). Leaf succulence is a distinctly drought avoidant trait associated with specialised leaf water storage tissues (Ogburn & Edwards, 2010; Vendramini et al., 2002). In mature *S. alba* leaves, a central region of non-photosynthetic water storage parenchyma cells account for approximately ~30% leaf thickness (Bryant, 2019), therefore acclimation of these specialised water storage cells may account for changing leaf p–v parameters. Expansion of the symplastic fraction enabled increased C_{leaf} while

TABLE 3 Estimates of water potentials inducing 12% (P_{12}), 50% (P_{50}), and 88% (P_{88}) loss of leaf hydraulic conductance (K_{leaf}), stomatal conductance (g_s) and stem hydraulic conductance (K_{stem}). Model parameters reflect slope at P_{50} (S_x) and 50% loss of conductance (P_x)

	Model parameters	Model estimates (MPa)			
	S_x	P_x	P_{12}	P_{50}	P_{88}
K_{leaf}	22.90	−2.36	−0.80 (0.14, 0.53)	−2.36 (−2.04, −2.65)	−4.83 (−4.09, −5.96)
g_s	44.69	−3.10	−2.03 (n/a)	−3.10 (−2.95, −3.25)	−4.10 (−4.09, n/a)
K_{stem}	31.32	−5.92	−4.27 (3.74, 5.92)	−5.92 (−5.41, −6.49)	−7.23 (−6.12, −8.09)

TABLE 4 Minimum water potential (Ψ_{min}) during the late dry season and hydraulic safety margins before loss of 50% hydraulic conductance (HSM_{50}) in leaves and stems. Dry season acclimation of water released from leaves in the canopy to buffer exposure to stem P_{50}

Parameter		Early dry season	Late dry season
Minimum water potential (MPa)	$\Psi_{min\ leaf}$	−2.66 ± 0.05	−3.62 ± 0.04**
	$\Psi_{min\ stem}$	−2.43 ± 0.03	−3.05 ± 0.07**
Minimum leaf RWC (%)	$RWC_{leaf\ at\ \Psi min}$	90.0 ± 1.6	76.0 ± 2.6**
Hydraulic safety margins	$HSM_{50\ leaf}$	−0.30 (−0.62,-0.01)	−1.26 (−0.93, −1.61)
	$HSM_{50\ stem}$	3.49 (2.98, 4.06)	2.87 (2.28, 3.51)
Leaf RWC at stem P_{50} (% RWC)	$RWC_{at\ stem\ P50}$	76.2 ± 2.8	48.1 ± 3.4**
Leaf symplastic RWC content at stem P_{50} (%)	$RWC_{symplast\ at\ stem\ P50}$	42.8 ± 1.6	39.3 ± 3.8 ns
Hydraulic safety margin to stem P_{50}:Ψ_{min} − $P_{50\ stem}$ (MPa)	$HSM_{50\ stem}$ (MPa)	3.84 (3.25, 4.48)	2.87 (2.28, 3.51)
$RWC_{leaf\ at\ \Psi min}$ - $RWC_{leaf\ at\ stem\ P50}$	$HSM_{50\ stem}$ (RWC)	13.8 ± 3.2	27.8 ± 4.3*
SWC × ($RWC_{leaf\ at\ \Psi min}$ - $RWC_{leaf\ at\ stem\ P50}$)	$HSM_{50\ stem}$ (leaf WC kg m^{-2})	0.063 ± 0.013	0.133 ± 0.015*

Note: Values are means ± SE, or means (95% upper CI, 95% lower CI).
Abbreviation: RWC, relative water content.

simultaneously buffering declines in $RWC_{symplast}$ with declining Ψ. Consequently, despite declining water potentials, no statistical differences were observed in leaf $RWC_{symplast\ at\ TLP}$ between early and late dry season, c. 76%, nor between leaf $RWC_{symplast}$ at water potentials associated with stem $P_{50.}$ As lethal limits of bulk leaf RWC are thought to be associated with membrane failure (Kursar et al., 2009; Tyree et al., 2003; Tyree, Cochard, Cruiziat, Sinclair, & Ameglio, 1993), conservation of relative symplastic volume under drought conditions reduces risk of exposure to critically low $RWC_{symplast}$ (Saliendra & Meinzer, 1991). While the bulk WC associated with leaf death reportedly varies between 40 and 70% between taxa and leaf types (Larcher, 2003), the capacity of some species to adjust apoplastic and symplastic distributions of bulk leaf water with declining water potentials, underlies whether species with low bulk RWC are actually tolerating or avoiding symplastic dehydration (Kozlowski & Pallardy, 2002). Indeed, our results highlight the importance of characterising declines in $RWC_{symplast}$, a value not often reported (Bartlett et al., 2012). Conservation of symplastic volume warrants future exploration in the characterization of acclimation to declines in Ψ and WC. As leaf area declined between early and late dry season, despite our sampling of only fully expanded leaves, the observed acclimation in leaf traits likely occurred in flushes of leaves developed during the dry season. We collected no data on the seasonality of leaf flushes and leaf lifespan, and the leaf longevity in this species remains unclear.

4.2 | Acclimation of π_{TLP} and C_{leaf} prolonged turgor and increased morning gas exchange

In general, drought reduces photosynthesis, primarily because early stomatal closure reduces intercellular CO_2 concentrations (Abrams & Kubiske, 1990; Epron & Dreyer, 1993; Flexas, Bota, Escalona, Sampol, & Medrano, 2002; Sack et al., 2003). Adjustment of π_{TLP} can delay stomatal closure and prolong gas exchange with declining Ψ (Brodribb, Holbrook, Edwards, & Gutiérrez, 2003). In *S. alba*, acclimation of π_{TLP} was required for sustained turgor with declining dry season plant water potentials; by late dry season $\Psi_{pd,}$ −2.67 ± 0.08 MPa, was only marginally distinct from the π_{TLP} in early dry season, −2.87 ± 0.05 MPa. Unexpectedly, we observed elevated midday photosynthetic rates in the late dry season and elevated stomatal conductance and transpiration rates early in the day with closure of stomata late in the day (Figure 2e,f). The potential role of increased C_{leaf} in these transient increases in *A* and gs, remains unclear. Notably, decreases in π_{TLP} coupled with the maintenance of SWC_{area} and a reduction in $A_{f,}$ increased the total leaf water released between full turgor and π_{TLP} by 90% and maintained the total stored water available for use between Ψ_{pd} and π_{TLP} at ~21 g m^{-2} (Table 1). While the latter accounts for only 6 min of average late dry season transpiration (3 mmol m^{-2} s^{-1}), in many species hydraulic capacitance and stored water buffer against

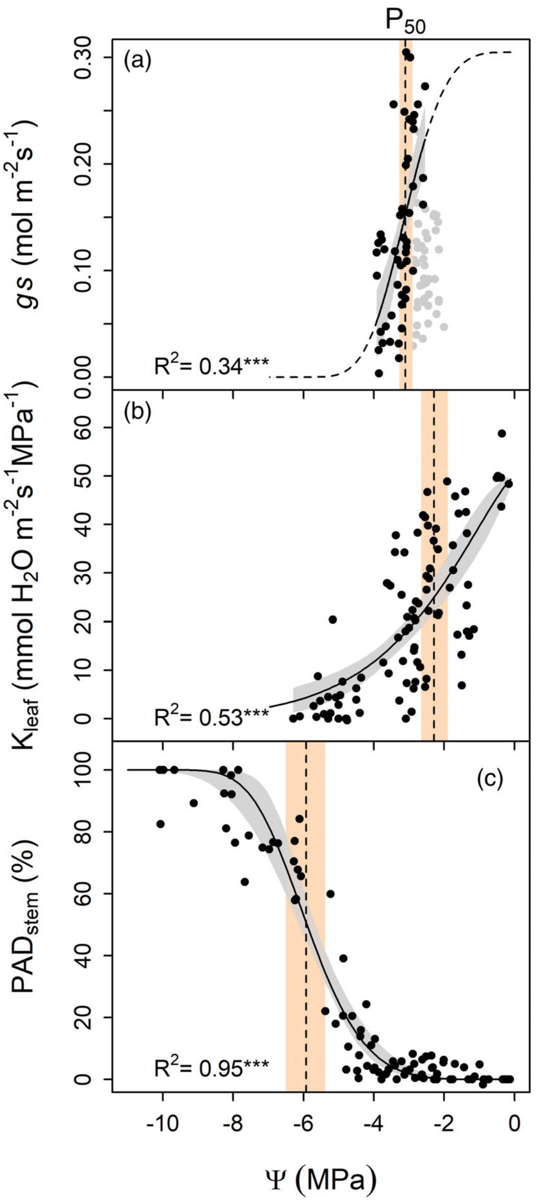

FIGURE 3 Response of conductance in (a) stomata, (b) leaves and (c) stems to declining water potential (Ψ). Stomatal conductance (g_s), leaf hydraulic conductance (K_{leaf}) and percent air discharge stem (PAD_{stem}). Curve depicts modelled percent loss of conductance, vertical lines depict estimates of water potentials inducing 50% loss of conductance (P_{50}). Shaded region depict bounds of 95% confidence interval. Grey points in panel (a) depict early dry season data not included in the analysis of g_s vulnerability. Significance codes: *** (p < .001). $n = 5–6$

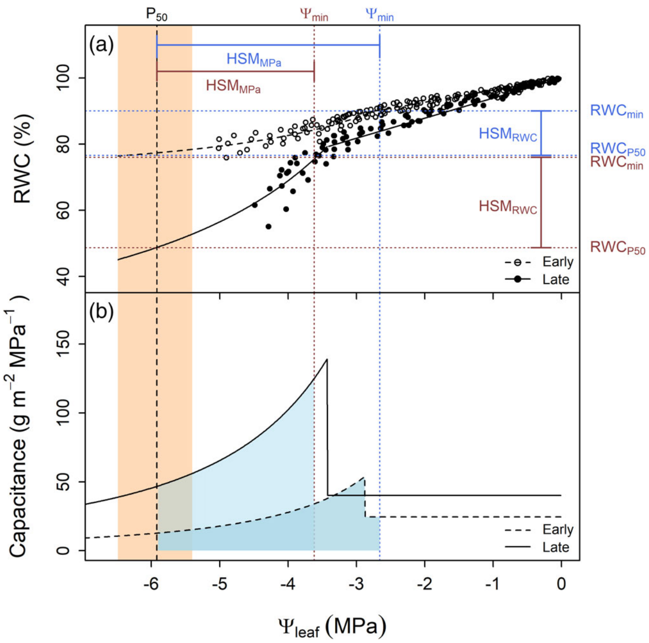

FIGURE 4 Late dry season increase in leaf capacitance and water released between minimum water potential (Ψ_{min}) and 50% stem embolism (P_{50}). (a) Leaf pressure-volume (p–v) plots from the early (open circles) and late dry season (closed circles). Points, depict pooled data from individuals ($n = 7$ in early dry season and $n = 6$ in late dry season). Trend lines depict the linear capacitance above leaf bulk turgor loss point and a non-linear capacitance below turgor loss point, as estimated from the linear region of a $1/\Psi_{leaf}$ plot. Black vertical line depicts water potential at 50% loss of stem hydraulic conductance (P_{50}), tan shaded region depicts a 95% CI. Vertical dotted lines depict observed minimum leaf water potential (Ψ_{min}) in the early (blue) and late dry seasons (red), and horizontal dotted lines depict RWC associated with Ψ_{min} (RWC_{min}) and stem P_{50} (RWC_{P50}). Vertical bars illustrate seasonal differences in the hydraulic safety margin between RWC_{min} and RWC_{P50}, that is, leaf water available for buffering excursions to water potentials associated with 50% loss of stem hydraulic conductance. (b) Dry season increase in instantaneous capacitance as a function Ψ_{leaf}, the derived slope of trendlines depicted in (a) in early (dashed line) and late (solid line) dry season. Capacitance above bulk turgor loss is constant, capacitance below turgor loss point increases sharply then declines with leaf dehydration. Shaded blue regions depict differences in leaf water release below Ψ_{min} for buffering excursions to water potentials associated with 50% loss of stem hydraulic conductance between the early (63.1 ± 12.7 g m^{-2}) and late dry season (133.2 ± 15.1 g m^{-2}) [Colour figure can be viewed at wileyonlinelibrary.com]

adverse water potentials gradients and stabilise tissue water potentials (Scholz et al., 2011). In *S. alba*, increased late dry season C_{leaf} offset a co-occurring reduction in stem capacitance, thereby maintaining overall shoot capacitance (Figure 1). Consequently, the necessity of increased C_{leaf} for the observed increases in morning stomatal conductance and elevated midday gas exchange in the late dry season cannot be ruled out.

4.3 | Shifting availability of leaf water within shoots conserved stem water content and increased stem hydraulic safety margins

In late dry season, reduced stem capacitance resulted in statistically insignificant amounts of water being discharged from the stem between full hydration and turgor loss (Table 2). Declines in stem water pools and hydraulic capacitance under drought conditions have been observed in several species (Beedlow, Waschmann, Lee, & Tingey, 2017; Hao, Wheeler, Holbrook, & Goldstein, 2013; Matheny et al., 2015; Salomón et al., 2020); however, our results suggest that by late dry season stem water content was highly conserved over the daily operational range, Ψ_{pd}-Ψ_{min}. While $HSM_{50\ stem}$ (MPa) in early and late dry season were not statistically different due to large confidence limits associated with stem P_{50} estimates, stem water potentials declined between early and late dry season, implying the predicted seasonal decline in $HSM_{50\ stem}$ (MPa). However, increased C_{leaf} following turgor loss resulted in a 111 ± 31% increase in the absolute leaf water content associated with $HSM_{50\ stem}$ (MPa), between early and late dry season. Counterintuitively, the potential contribution of leaf water to preservation of stem function was greatest during the driest time of the year (Figure 4, Table 4). While we do not have an estimate for shoot water content corresponding to HSM_{50} for early and late dry season, the similarity in C_{shoot} between early and late dry season suggests that the shoot water content associated with this margin may not have changed seasonally. Shifting hydraulic capacitance of leaves and stems, as observed in *S. alba*, may underpin previous findings of relocation of leaf-water in *Maesopsis eminii* shoots from leaves to stems, suggesting that leaf water buffers exposure of stems to water potentials associated with critical loss of hydraulic conductance (Epila et al., 2017). Leaf capacitance has been conventionally characterized over the functional range preceding turgor loss where it is largely linear; however, the dramatic increase in C_{leaf} following turgor loss appears to provide a significant stabilising effect for further declines in Ψ for leaves and stems alike and warrants exploration in future studies (Bartlett et al., 2012).

Our results also highlight the potential interaction between differential organ capacitance and hydraulic segmentation. Recent tests of the hydraulic segmentation hypothesis (Zimmerman, 1983) have yielded mixed results among species' and biomes (Li et al., 2020; Pivovaroff, Sack, & Santiago, 2014; Skelton, Brodribb, & Choat, 2017). Consistent with hydraulic segmentation, we observed smaller hydraulic safety margins in leaves than stems (Figure 3, Table 4). Our results are consistent with predictions that hydraulic segmentation is more likely in tropical trees experiencing wet-dry monsoonal seasonality, relative to tropical trees experiencing a tropical rainforest climate, that is, homogenous distribution of rainfall (Bucci, Goldstein, Scholz, & Meinzer, 2016). Differential hydraulic capacitance in leaves and stems combined with segmentation of hydraulic vulnerability, predict that under intensified drought stress *S. alba* may rely on reducing evaporative surface area through leaf shedding to preserve stem hydraulic function.

Our observation of shifting use and availability of water pools in *S. alba* illustrates that despite the utility of indexing HSM_{50} in units of MPa, as has been the convention (Choat et al., 2012), the absolute water content associated with these margins and its accessibility is critical in determining drought risk, yet poorly understood (Blackman et al., 2016). Our findings support recent emphasis on the importance of assessing vulnerability to drought and mortality via tissue WC (Gleason et al., 2014; Körner, 2019; Martinez-Vilalta et al., 2019; McCulloh et al., 2014; Sapes et al., 2019). Further, the seasonal acclimation of the A_f observed in *S. alba* highlights limitations of investigating declining bulk tissue WC without reference to its significance for $RWC_{symplast}$. Our results affirm the value of future research linking declining Ψ to declining WC and loss of membrane integrity in characterization of drought-induced plant mortality and potential recovery (John, Henry, & Sack, 2018; Mantova, Menezes-Silva, Badel, Cochard, & Torres-Ruiz, 2021; Vilagrosa et al., 2010).

5 | CONCLUSIONS

Our results highlight the importance of increasing atmospheric drought in driving acclimation, plant productivity declines and mortality (de Cárcer et al., 2018; Eamus, Boulain, Cleverly, & Breshears, 2013; Grossiord et al., 2020; Yuan et al., 2019), particularly in the wet-dry tropics where intensifications of seasonality portend increased dry season aridity in coming decades (Chou et al., 2013). We identified a strategy of desiccation tolerance in *S. alba* involving maintenance of turgor, gas exchange and hydraulic conductance with declining tissue Ψ in the late dry season; however, late dry season acclimation also enhanced desiccation and dehydration avoidance. By increasing the contribution of C_{leaf} to shoot capacitance while shifting access to pools of water within leaves, *S. alba* avoided further declines in Ψ and leaf $RWC_{symplast}$. The present study highlights the central roles of hydraulic capacitance and shifting availability of pools of shoot water in mitigating the twin risks of carbon depletion and hydraulic failure under drought conditions.

ACKNOWLEDGEMENTS

Research was conducted with financial support from Australian Research Council Discovery Grant DP180102969 awarded to M.B., L.S. and M.M. CB was supported by an Australian Government Research Training Program (RTP) Scholarship. TIF was supported by the Becas Chile PhD scholarship program granted by ANID. OB was supported by Australian Research Council Discovery Grant DP170104091. We thank Catherine Bone for outstanding support of field work conducted in mangrove forest along the Daintree River.

CONFLICT OF INTEREST

The authors declare there is no conflict of interest.

AUTHOR CONTRIBUTIONS

Callum Bryant and Marilyn C. Ball: Conceived the study and designed the experiments. **Callum Bryant, Nigel Brothers, and Tomas I. Fuenzalida**: Collected the data. **Callum Bryant**: Analysed the data with suggestions from Marilyn C. Ball, Tomas I. Fuenzalida, Oliver Binks, Lawren Sack, Maurizio Mencuccini. **Callum Bryant**: Wrote the manuscript with input from Tomas I. Fuenzalida, Nigel Brothers, Lawren Sack, Maurizio Mencuccini, Oliver Binks and Marilyn C. Ball.

DATA AVAILABILITY STATEMENT

The data that support the findings of this study are openly available in ANU Data Commons at https://dx.doi.org/10.25911/608ba2e1921bc, reference number anudc:6096.

ORCID

Callum Bryant https://orcid.org/0000-0002-8035-9157
Tomas I. Fuenzalida https://orcid.org/0000-0002-8353-5080
Lawren Sack https://orcid.org/0000-0002-7009-7202
Oliver Binks https://orcid.org/0000-0002-6291-3644

REFERENCES

Abrams, M. D., & Kubiske, M. E. (1990). Photosynthesis and water relations during drought in *Acer rubrum* L. genotypes from contrasting sites in Central Pennsylvania. *Functional Ecology*, *4*, 727–733.

Adams, H. D., Zeppel, M. J. B., Anderegg, W. R. L., Hartmann, H., Landhäusser, S. M., Tissue, D. T., … McDowell, N. G. (2017). A multi-species synthesis of physiological mechanisms in drought-induced tree mortality. *Nature Ecology & Evolution*, *1*, 1285–1291.

Allen, C. D., & Breshears, D. D. (2007). Climate-induced forest dieback as an emergent global phenomenon. *Eos, Transactions American Geophysical Union*, *88*, 504–504.

Allen, C. D., Breshears, D. D., & McDowell, N. G. (2015). On underestimation of global vulnerability to tree mortality and forest die-off from hotter drought in the Anthropocene. *Ecosphere*, *6*, 1–55.

Anderegg, W. R. L., Klein, T., Bartlett, M., Sack, L., Pellegrini, A. F. A., Choat, B., & Jansen, S. (2016). Meta-analysis reveals that hydraulic traits explain cross-species patterns of drought-induced tree mortality across the globe. *Proceedings of the National Academy of Sciences of the United States of America*, *113*, 5024–5029.

Ball, M. C., & Pidsley, S. M. (1995). Growth responses to salinity in relation to distribution of two mangrove species, *Sonneratia alba* and *S. lanceolata*, in northern Australia. *Functional Ecology*, *9*, 77–85.

Bartlett, M. K., Detto, M., & Pacala, S. W. (2019). Predicting shifts in the functional composition of tropical forests under increased drought and CO_2 from trade-offs among plant hydraulic traits. *Ecology Letters*, *22*, 67–77.

Bartlett, M. K., Klein, T., Jansen, S., Choat, B., & Sack, L. (2016). The correlations and sequence of plant stomatal, hydraulic, and wilting responses to drought. *Proceedings of the National Academy of Sciences of the United States of America*, *113*, 13098–13103.

Bartlett, M. K., Scoffoni, C., & Sack, L. (2012). The determinants of leaf turgor loss point and prediction of drought tolerance of species and biomes: A global meta-analysis. *Ecology Letters*, *15*, 393–405.

Bartlett, M. K., Zhang, Y., Kreidler, N., Sun, S., Ardy, R., Cao, K., & Sack, L. (2014). Global analysis of plasticity in turgor loss point, a key drought tolerance trait. *Ecology Letters*, *17*, 1580–1590.

Beedlow, P. A., Waschmann, R. S., Lee, E. H., & Tingey, D. T. (2017). Seasonal patterns of bole water content in old growth Douglas-fir (*Pseudotsuga menziesii* [Mirb.] Franco). *Agricultural and Forest Meteorology*, *242*, 109–119.

Binks, O., Meir, P., Rowland, L., da Costa, A. C. L., Vasconcelos, S. S., de Oliveira, A. A. R., … Mencuccini, M. (2016). Plasticity in leaf-level water relations of tropical rainforest trees in response to experimental drought. *New Phytologist*, *211*, 477–488.

Blackman, C. J., Pfautsch, S., Choat, B., Delzon, S., Gleason, S. M., & Duursma, R. A. (2016). Toward an index of desiccation time to tree mortality under drought. *Plant, Cell & Environment*, *39*, 2342–2345.

Brodribb, T. J., & Holbrook, N. M. (2003). Stomatal closure during leaf dehydration, correlation with other leaf physiological traits. *Plant Physiology*, *132*, 2166–2173.

Brodribb, T. J., Holbrook, N. M., Edwards, E. J., & Gutiérrez, M. V. (2003). Relations between stomatal closure, leaf turgor and xylem vulnerability in eight tropical dry forest trees. *Plant, Cell & Environment*, *26*, 443–450.

Brodribb, T. J., Powers, J., Cochard, H., & Choat, B. (2020). Hanging by a thread? Forests and drought. *Science*, *368*, 261–266.

Bryant C. (2019). Foliar surface water uptake and hydraulic function in the mangrove, *Sonneratia alba* (Honours thesis). Australian National University.

Bucci, S. J., Goldstein, G., Scholz, F. G., & Meinzer, F. C. (2016). Physiological significance of hydraulic segmentation, nocturnal transpiration and capacitance in tropical trees: Paradigms revisited. In G. Goldstein & L. S. Santiago (Eds.), *Tropical tree physiology: Adaptations and responses in a changing environment* (pp. 205–225). Cham: Springer International Publishing.

Carrasco, L. O., Bucci, S. J., Di Francescantonio, D., Lezcano, O. A., Campanello, P. I., Scholz, F. G., … Goldstein, G. (2015). Water storage dynamics in the main stem of subtropical tree species differing in wood density, growth rate and life history traits. *Tree Physiology*, *35*, 354–365.

Chimenti, C. A., & Hall, A. J. (1994). Responses to water stress of apoplastic water fraction and bulk modulus of elasticity in sunflower (*Helianthus annuus* L.) genotypes of contrasting capacity for osmotic adjustment. *Plant and Soil*, *166*, 101–107.

Choat, B., Jansen, S., Brodribb, T. J., Cochard, H., Delzon, S., Bhaskar, R., … Zanne, A. E. (2012). Global convergence in the vulnerability of forests to drought. *Nature*, *491*, 752–755.

Chou, C., Chiang, J. C. H., Lan, C.-W., Chung, C.-H., Liao, Y.-C., & Lee, C.-J. (2013). Increase in the range between wet and dry season precipitation. *Nature Geoscience*, *6*, 263–267.

Davy, R., Esau, I., Chernokulsky, A., Outten, S., & Zilitinkevich, S. (2017). Diurnal asymmetry to the observed global warming. *International Journal of Climatology*, *37*, 79–93.

de Cárcer, P. S., Vitasse, Y., Peñuelas, J., Jassey, V. E. J., Buttler, A., & Signarbieux, C. (2018). Vapor–pressure deficit and extreme climatic variables limit tree growth. *Global Change Biology*, *24*, 1108–1122.

Duke, N., Ball, M., & Ellison, J. (1998). Factors influencing biodiversity and distributional gradients in mangroves. *Global Ecology & Biogeography Letters*, *7*, 27–47.

Duursma, R. A., Blackman, C. J., Lopéz, R., Martin-StPaul, N. K., Cochard, H., & Medlyn, B. E. (2019). On the minimum leaf conductance: Its role in models of plant water use, and ecological and environmental controls. *New Phytologist*, *221*, 693–705.

Eamus, D., Boulain, N., Cleverly, J., & Breshears, D. D. (2013). Global change-type drought-induced tree mortality: Vapor pressure deficit is more important than temperature per se in causing decline in tree health. *Ecology and Evolution*, *3*, 2711–2729.

Epila, J., De Baerdemaeker, N. J. F., Vergeynst, L. L., Maes, W. H., Beeckman, H., & Steppe, K. (2017). Capacitive water release and internal leaf water relocation delay drought-induced cavitation in African *Maesopsis eminii*. *Tree Physiology*, *37*, 481–490.

Epron, D., & Dreyer, E. (1993). Long-term effects of drought on photosynthesis of adult oak trees [*Quercus petraea* (Matt.) Liebl. and *Quercus robur* L.] in a natural stand. *New Phytologist*, *125*, 381–389.

Ewers, F. W. & Fisher, J. B. (1989). Techniques for measuring vessel lengths and diameters in stems of woody plants. *American Journal of Botany*, *76*, 645–656.

Ficklin, D. L., & Novick, K. A. (2017). Historic and projected changes in vapor pressure deficit suggest a continental-scale drying of the United States atmosphere. *Journal of Geophysical Research: Atmospheres*, *122*, 2061–2079.

Flexas, J., Bota, J., Escalona, J. M., Sampol, B., & Medrano, H. (2002). Effects of drought on photosynthesis in grapevines under field conditions: An evaluation of stomatal and mesophyll limitations. *Functional Plant Biology*, *29*, 461–471.

Gleason, S. M., Blackman, C. J., Cook, A. M., Laws, C. A., & Westoby, M. (2014). Whole-plant capacitance, embolism resistance and slow transpiration rates all contribute to longer desiccation times in woody angiosperms from arid and wet habitats. *Tree Physiology*, *34*, 275–284.

Grossiord, C., Buckley, T. N., Cernusak, L. A., Novick, K. A., Poulter, B., Siegwolf, R. T. W., … McDowell, N. G. (2020). Plant responses to rising vapor pressure deficit. *New Phytologist*, *226*, 1550–1566.

Hao, G.-Y., Sack, L., Wang, A.-Y., Cao, K.-F., & Goldstein, G. (2010). Differentiation of leaf water flux and drought tolerance traits in hemiepiphytic and non-hemiepiphytic Ficus tree species. *Functional Ecology*, *24*, 731–740.

Hao, G.-Y., Wheeler, J. K., Holbrook, N. M., & Goldstein, G. (2013). Investigating xylem embolism formation, refilling and water storage in tree trunks using frequency domain reflectometry. *Journal of Experimental Botany*, *64*, 2321–2332.

Harvey, H. W. (1966). *The chemistry and fertility of sea waters*. Cambridge: Cambridge University Press.

Hochberg, U., Albuquerque, C., Rachmilevitch, S., Cochard, H., David-Schwartz, R., Brodersen, C. R., … Windt, C. W. (2016). Grapevine petioles are more sensitive to drought induced embolism than stems: Evidence from in vivo MRI and microcomputed tomography observations of hydraulic vulnerability segmentation. *Plant, Cell & Environment*, *39*, 1886–1894.

Hsiao, T. C. (1973). Plant responses to water stress. *Ann Rev. Plant Physiology*, *24*, 519–570.

John, G. P., Henry, C., & Sack, L. (2018). Leaf rehydration capacity: Associations with other indices of drought tolerance and environment. *Plant, Cell & Environment*, *41*, 2638–2653.

Joly, R. J., & Zaerr, J. B. (1987). Alteration of cell-wall water content and elasticity in Douglas-Fir during periods of water deficit. *Plant Physiology*, *83*, 418–422.

Kerstiens, G. (1996). Cuticular water permeability and its physiological significance. *Journal of Experimental Botany*, *47*, 1813–1832.

Körner, C. (2019). No need for pipes when the well is dry—A comment on hydraulic failure in trees. *Tree Physiology*, *39*, 695–700.

Kozlowski, T. T., & Pallardy, S. G. (1997). *Physiology of woody plants* (2nd ed.). San Diego, CA: Academic Press.

Kozlowski, T. T., & Pallardy, S. G. (2002). Acclimation and adaptive responses of woody plants to environmental stresses. *The Botanical Review*, *68*, 270–334.

Kursar, T. A., Engelbrecht, B. M. J., Burke, A., Tyree, M. T., Omari, B. E., & Giraldo, J. P. (2009). Tolerance to low leaf water status of tropical tree seedlings is related to drought performance and distribution. *Functional Ecology*, *23*, 93–102.

Larcher, W. (2003). *Physiological plant ecology: Ecophysiology and stress physiology of functional groups*. Berlin, Heidelberg: Springer Science & Business Media.

Li, X., Delzon, S., Torres-Ruiz, J., Badel, E., Burlett, R., Cochard, H., … Choat, B. (2020). Lack of vulnerability segmentation in four angiosperm tree species: Evidence from direct X-ray microtomography observation. *Annals of Forest Science*, *77*, 37.

Mantova, M., Menezes-Silva, P. E., Badel, E., Cochard, H., & Torres-Ruiz, J. M. (2021). The interplay of hydraulic failure and cell vitality explains tree capacity to recover from drought. *Physiologia Plantarum*, *172*, 247–257.

Martinez-Vilalta, J., Anderegg, W. R. L., Sapes, G., & Sala, A. (2019). Greater focus on water pools may improve our ability to understand and anticipate drought-induced mortality in plants. *New Phytologist*, *223*, 22–32.

Matheny, A. M., Bohrer, G., Garrity, S. R., Morin, T. H., Howard, C. J., & Vogel, C. S. (2015). Observations of stem water storage in trees of opposing hydraulic strategies. *Ecosphere*, *6*, art165.

Maury, P., Berger, M., Mojayad, F., & Planchon, C. (2000). Leaf water characteristics and drought acclimation in sunflower genotypes. *Plant and Soil*, *223*, 155–162.

McCulloh, K. A., Johnson, D. M., Meinzer, F. C., & Woodruff, D. R. (2014). The dynamic pipeline: Hydraulic capacitance and xylem hydraulic safety in four tall conifer species. *Plant, Cell & Environment*, *37*, 1171–1183.

Meehl, G. A., & Tebaldi, C. (2004). More intense, more frequent, and longer lasting heat waves in the 21st century. *Science*, *305*, 994–997.

Meinzer, F. C., Johnson, D. M., Lachenbruch, B., McCulloh, K. A., & Woodruff, D. R. (2009). Xylem hydraulic safety margins in woody plants: Coordination of stomatal control of xylem tension with hydraulic capacitance. *Functional Ecology*, *23*, 922–930.

Melcher, P. J., Meinzer, F. C., Yount, D. E., Goldstein, G., & Zimmermann, U. (1998). Comparative measurements of xylem pressure in transpiring and non-transpiring leaves by means of the pressure chamber and the xylem pressure probe. *Journal of Experimental Botany*, *49*, 1757–1760.

Nguyen, H. T., Meir, P., Sack, L., Evans, J. R., Oliveira, R. S., & Ball, M. C. (2017). Leaf water storage increases with salinity and aridity in the mangrove *Avicennia marina*: Integration of leaf structure, osmotic adjustment and access to multiple water sources. *Plant, Cell & Environment*, *40*, 1576–1591.

Ogburn, R. M., & Edwards, E. J. (2010). Chapter 4 - the ecological water-use strategies of succulent plants. In J.-C. Kader & M. Delseny (Eds.), *Advances in Botanical Research* (pp. 179–225). Cambridge, Massachusetts: Academic Press.

Ogle, K., Barber, J. J., Willson, C., & Thompson, B. (2009). Hierarchical statistical modeling of xylem vulnerability to cavitation. *New Phytologist*, *182*, 541–554.

Pearcy, R., Schulze, E. & Zimmermann, R. (2000). Measurement of transpiration and leaf conductance. In Pearcy, R. Ehlering, J., Mooney, H., & Rundel, P (Eds.), *Plant physiological ecology* (pp. 137–160). Dordrecht: Springer.

Pereira, L., Bittencourt, P. R. L., Oliveira, R. S., Junior, M. B. M., Barros, F. V., Ribeiro, R. V., & Mazzafera, P. (2016). Plant pneumatics: Stem air flow is related to embolism – New perspectives on methods in plant hydraulics. *New Phytologist*, *211*, 357–370.

Pivovaroff, A. L., Sack, L., & Santiago, L. S. (2014). Coordination of stem and leaf hydraulic conductance in southern California shrubs: A test of the hydraulic segmentation hypothesis. *New Phytologist*, *203*, 842–850.

Rodriguez-Dominguez, C. M., Murphy, M. R. C., Lucani, C., & Brodribb, T. J. (2018). Mapping xylem failure in disparate organs of whole plants reveals extreme resistance in olive roots. *New Phytologist*, *218*, 1025–1035.

R Core Team (2019). R: A language and environment for statistical computing. R Foundation for Statistical Computing, Vienna, Austria. URL http://www.R-project.org/.

Rosas, T., Mencuccini, M., Barba, J., Cochard, H., Saura-Mas, S., & Martínez-Vilalta, J. (2019). Adjustments and coordination of hydraulic, leaf and stem traits along a water availability gradient. *New Phytologist*, *223*, 632–646.

Sack, L., Cowan, P. D., Jaikumar, N., & Holbrook, N. M. (2003). The 'hydrology' of leaves: Co-ordination of structure and function in temperate woody species. *Plant, Cell & Environment*, *26*, 1343–1356.

Sack, L., Medeiros, C. D., Scoffoni, C., John, G. P., Bartlett, M. K., Inman-Narahari, F., … Price, J. (2018). Using a broad suite of traits, including hydraulics, for robust prediction of species and forest vital rates in space and time. *AGU Fall Meeting Abstracts*, *2018*, B11B–B2146B.

Saliendra, N. Z., & Meinzer, F. C. (1991). Symplast volume, turgor, stomatal conductance and growth in relation to osmotic and elastic adjustment in droughted sugarcane. *Journal of Experimental Botany*, *42*, 1251–1259.

Salomón, R. L., Steppe, K., Ourcival, J. M., Villers, S., Rodríguez-Calcerrada, J., Schapman, R., & Limousin, J. M. (2020). Hydraulic acclimation in a Mediterranean oak subjected to permanent throughfall exclusion results in increased stem hydraulic capacitance. *Plant, Cell & Environment*, *43*, 1528–1544.

Sanders, G. J., & Arndt, S. K. (2012). Osmotic adjustment under drought conditions. In R. Aroca (Ed.), *Plant responses to drought stress*. Berlin, Heidelberg: Springer.

Sapes, G., Roskilly, B., Dobrowski, S., Maneta, M., Anderegg, W. R. L., Martinez-Vilalta, J., & Sala, A. (2019). Plant water content integrates hydraulics and carbon depletion to predict drought-induced seedling mortality. *Tree Physiology*, *39*, 1300–1312.

Scholz, F. G., Phillips, N. G., Bucci, S. J., Meinzer, F. C., & Goldstein, G. (2011). Hydraulic capacitance: Biophysics and functional significance of internal water sources in relation to tree size. In F. C. Meinzer, B. Lachenbruch, & T. E. Dawson (Eds.), *Size- and age-related changes in tree structure and function* (pp. 341–361). Dordrecht, the Netherlands: Springer Netherlands.

Skelton, R. P., Brodribb, T. J., & Choat, B. (2017). Casting light on xylem vulnerability in an herbaceous species reveals a lack of segmentation. *New Phytologist*, *214*, 561–569.

Trenberth, K. E., Dai, A., van der Schrier, G., Jones, P. D., Barichivich, J., Briffa, K. R., & Sheffield, J. (2014). Global warming and changes in drought. *Nature Climate Change*, *4*, 17–22.

Tsuda, M., & Tyree, M. T. (1997). Whole-plant hydraulic resistance and vulnerability segmentation in *Acer saccharinum*. *Tree Physiology*, *17*, 351–357.

Tyree, M. T., Cochard, H., Cruiziat, P., Sinclair, B., & Ameglio, T. (1993). Drought-induced leaf shedding in walnut: Evidence for vulnerability segmentation. *Plant, Cell & Environment*, *16*, 879–882.

Tyree, M. T., Engelbrecht, B. M. J., Vargas, G., & Kursar, T. A. (2003). Desiccation tolerance of five tropical seedlings in Panama. Relationship to a field assessment of drought performance. *Plant Physiology*, *132*, 1439–1447.

Tyree, M. T., & Hammel, H. T. (1972). The measurement of the turgor pressure and the water relations of plants by the pressure-bomb technique. *Journal of Experimental Botany*, *23*, 267–282.

Vendramini, F., Díaz, S., Gurvich, D. E., Wilson, P. J., Thompson, K., & Hodgson, J. G. (2002). Leaf traits as indicators of resource-use strategy in floras with succulent species. *New Phytologist*, *154*, 147–157.

Vilagrosa, A., Morales, F., Abadía, A., Bellot, J., Cochard, H., & Gil-Pelegrin, E. (2010). Are symplast tolerance to intense drought conditions and xylem vulnerability to cavitation coordinated? An integrated analysis of photosynthetic, hydraulic and leaf level processes in two Mediterranean drought-resistant species. *Environmental and Experimental Botany*, *69*, 233–242.

Wolf, A., Anderegg, W. R. L., & Pacala, S. W. (2016). Optimal stomatal behavior with competition for water and risk of hydraulic impairment. *Proceedings of the National Academy of Sciences of the United States of America*, *113*, E7222–E7230.

Yuan, W., Zheng, Y., Piao, S., Ciais, P., Lombardozzi, D., Wang, Y., … Yang, S. (2019). Increased atmospheric vapor pressure deficit reduces global vegetation growth. *Science Advances*, *5*, eaax1396.

Zhang, Y., Lamarque, L. J., Torres-Ruiz, J. M., Schuldt, B., Karimi, Z., Li, S., … Jansen, S. (2018). Testing the plant pneumatic method to estimate xylem embolism resistance in stems of temperate trees. *Tree Physiology*, *38*, 1016–1025.

Zimmerman, M. (1983). *Xylem structure and the ascent of sap*. Berlin: Springer Science & Business Media.

SUPPORTING INFORMATION

Additional supporting information may be found online in the Supporting Information section at the end of this article.

How to cite this article: Bryant, C., Fuenzalida, T. I., Brothers, N., Mencuccini, M., Sack, L., Binks, O., & Ball, M. C. (2021). Shifting access to pools of shoot water sustains gas exchange and increases stem hydraulic safety during seasonal atmospheric drought. *Plant, Cell & Environment*, *44*(9), 2898–2911. https://doi.org/10.1111/pce.14080